Remediation of pear iron chlorosis by nanocellulose-iron chelation and mechanisms

Hezhong Wang (hezhongw@126.com)

Research

Keywords: Nanocrystal cellulose, Nanocellulose-iron chelation, Iron chlorosis, Photosynthesis, Gene expression regulation

Posted Date: September 24th, 2021

DOI: https://doi.org/10.21203/rs.3.rs-934187/v1

Abstract

Background: Nanocrystal cellulose has a strong ability to chelate iron and the nanocomposite possesses strong adsorptive property. Iron deficiency chlorosis (IDC) is a mineral disorder that weakens pear photosynthesis and cause a significant decline in plant yield and quality. Conventional methods to control IDC are generally due to low efficiency and overuse of chemicals. The purpose of this study was to explore the capability of nanocellulose (NC)-Fe chelate to remediate pear IDC. Acidic hydrolyzed NCs were chelated with Fe (NCFe) based on the net charge density of the components. Foliar application of NCFe was employed to pre-etiolated seedlings of *Pyrus betulifolia* as a plant material. The ability of NCFe to promote active iron content (C_{Fe}), photosynthesis rate, and relative gene expression was studied.

Results: Nanocrystal cellulose prepared by acidic hydrolysis exhibit rod-like whiskers carrying on negative charges. When NCs were mixed with $FeSO_4$, the NCFe particles maintained a small, whisker-like morphology with small dots (Fe) on the surface of the NC particles. The Z-average hydrodynamic diameter and zeta potential of the NC whiskers measured by DLS were 84.3 ± 0.2 nm and -47.3 ± 1.7 mV, respectively. The particle size and zeta potential of NCFe were 107.4±3.0 nm and -9.7±0.4 mV, respectively. The results showed that NCFe could significantly mitigate IDC in seedlings by increasing C_{Fe}, photosynthesis parameters, major physiological indicators, and regulating the expression of key enzymes. When NCFe was prepared at a NC-to-Fe charge density ratio of 1:3,000, C_{Fe} and chlorophyll contents were enhanced by approximately 9 times and 72.7%, respectively; the major physiological indicators were all significantly increased. Interestingly, NCFe treatment significantly downregulated the expression of the pectin methylesterase gene (*PbPME*) and upregulated the expression of the ferritin gene (*PbFER*) to increase C_{Fe}.

Conclusion: NCs have strong potential to promote plant photosynthesis when chelated with Fe. The remediation capability of NCFe to IDC is attributed to the enhancement of photosynthesis parameters and indicators. NCFe treatment significantly downregulated the expression of the PME gene (*PbPME*) and upregulated the expression of the ferritin gene (*PbFER*) to increase the active iron content. This finding will provide a good alternative and a complementary strategy for Fe-chelate applications in plant iron chlorosis management.

Introduction

Iron (Fe) plays important roles in several basic physiological functions and is an important factor for pear tree growth and development. Fe deficiency chlorosis (IDC) became a worldwide problem starting in the 1930s, particularly in semiarid regions containing calcareous soils [1]. Since then, IDC has been reported in many varieties of *Pyrus communis* cv. in different regions [2–5]. The IDC of pear trees decreases not only the leaf chlorophyll content, active iron content, and photosynthetic capacity but also the yield and quality of pear products [6, 7]. Studies have demonstrated that nutrient absorption by leaves is usually quicker and more efficient than that through roots, especially at a high soil pH and calcium carbonate content [8]. Foliar application of $FeSO_4$, Fe-EDTA, or Fe-ethylene diamine-N,N'-bis(hydroxy phenyl)acetic

acid (EDDHA) is a conventional method to correct iron chlorosis in pear trees [8]; however, synthetic Fe-EDTA and Fe-EDDHA are expensive and contain significant amounts of potential pollutants, which risks environmental safety [9]. Although the cost of spraying $FeSO_4$ is relatively low, Fe(II) salts are rapidly oxidized upon exposure to ambient air and cannot fully control the IDC of pear trees [10].

Ferritin is a ubiquitous protein found in all cells, where its principal function appears to be the storage of iron in leaves [11]. Chlorophyll and carotenoids are essential pigments in photosynthesis. Carotenoids absorb light in the blue-green region and are able to transfer this excitation energy to chlorophyll and promote photosynthesis [12]. On the other hand, pectin is one of the main components of the cell wall, existing as a methylated ester of d-galacturonic acid, and exhibits strong affinity to bind cellulose nanocrystals (NCs) [13]. Relatively high pectin methylesterase (PME) activity promotes the demethylation of pectin, alters the degree and pattern of methyl esterification and releases methanol and protons, thus affecting plant cell wall integrity and rigidity [14]. In calcareous soil, the pH of plant leaf apoplasts is relatively high, promoting ferrous iron oxidation and fixation [15]. Therefore, it is necessary to develop new and environmentally friendly iron chelating agents to improve the absorption of foliar-applied Fe or enhance its translocation efficiency from source to sink tissue [16].

The integration of nanotechnology and biotechnology allows for the development of new solutions to agricultural sustainability. Nanofertilizers and nanopesticides have been of growing interest in the agriculture and food sectors in recent years [17, 18]. Cellulose is one of the most abundant materials in nature, and NCs have recently brought scientific and economic interest to the research community. The advanced characteristics of NCs are attributed to their small size, high surface area, and polyionic mechanical stiffness. Studies have shown that wood cellulose-based polyelectrolyte nanocomplexes can be used as novel carriers for protein delivery systems in agriculture [19, 20] and in environmental remediation as bioadsorbents [21, 22]. NC–iron oxide composites could be used as DNA electrochemical biosensors to detect *Mycobacterium tuberculosis* [23]. Most recently, Baruah et al. [24] studied nanocellulose-iron oxide nanobiocomposites remediating contaminated groundwater and found that this nanocomposite possessed strong adsorptive properties and magnetic recoverability. However, as a comprehensive bionanomaterial, carbon nanocellulose-iron chelate (NCFe) has not yet been systematically studied in agriculture. The objective of this research was to investigate the effectiveness of NCFe in promoting the uptake and activation of iron and promoting photosynthesis to remediate IDC and briefly discuss the underlying molecular mechanism. In this study, NCFe formulations were prepared based on the net charge density in an aqueous solution, and the effects of NCFe on chlorophyll, activation of iron, photosynthesis parameters, and relative gene expression were investigated. The brief molecular mechanism of iron activation induced by NCFe in IDC plants was revealed.

Experimental

Materials

Cellulose, in the form of dissolving-grade softwood sulfite pulp (Temalfa 95A), was kindly provided by Rayonier Advanced Materials Company (Temiscaming, Québec, Canada). Sulfuric acid (95–98%) was purchased from Haohua Chemical Company (Henan, China), and hydrochloric acid (36–38%) was purchased from Shuangshuang Chemical Company (Shandong, China). Ferrous sulfate and EDTA-Fe(III) were purchased from BBI Life Sciences Corporation (BBI CO., Inc. Shanghai, China). Deionized water (DI water) was used in the experiments, which was prepared with a Millipore Direct-Q 5 ultrapure water system. All other chemicals used were of analytical grade.

Preparation and characterization of nanocellulose

Nanocellulose suspensions (NCs) were prepared by acidic hydrolysis following Dong's method [25] with some minor modifications. Briefly, 20 g of cellulose powder milled in a universal grinder (FW100, Taisite Instrument Company, Tianjin, China) was hydrolyzed in 200 mL of 64 wt% H_2SO_4 under stirring at 45°C for 45 min. Then, 500 mL of precooled DI water (4°C) was added to stop the reaction. The pellet was collected by centrifugation at 9000 rpm and 4°C for 15 min. The reaction was repeated three times under the same hydrolysis conditions. The final product was washed three times and redispersed in 200 mL of DI water and dialyzed against DI water in dialysis tubing (JMD45-12∼14-0.5, Solarbio) to remove the acid residue until the pH of the dialysis water remained constant (pH = 5.4 ± 0.3).

The obtained suspension from dialysis was then sonicated in an ice bath for 25 min (5 s/5 s) at 35% output with an ultrasonic processor (JY98-IIIN, Ningbo Scientz Biotechnology Co., Ltd, Ningbo, China) to break down aggregates. Finally, the suspension was subsequently filtered through 1.0 μm and 0.45 μm PVDF syringe filters. The stock suspension was stored at 4°C for future use.

The concentration of the NC product was determined in triplicate from the weight difference of a 3 mL aliquot before and after drying for 2 h in an oven at 80°C. The net charge density of the NC suspension and ferrous sulfate solution was determined in triplicate by conductometric titration using a Mettler Toledo S470-USP/EP pH/conductivity meter with an In Lab 730 conductivity probe (Mettler Toledo International Co., Ltd. Zurich, Switzerland) following the method described by Wang and Roman [26]. Briefly, 25 mL of the stock suspension of NCs was titrated with 0.02 M NaOH by 100 μL increments of the titrant under stirring. Before titration, the ionic strength of the sample was adjusted to 0.01 mM using 5 M NaCl. The interval pH and conductivity values of the sample were recorded when the meter showed a stable reading. Based on the equivalence points of each range of the conductivity plot, the net charge density was calculated from the titrant volume consumed to neutralize counterions in the system.

The NCs were characterized by transmission electron microscopy (TEM), dynamic light scattering (DLS), and conductometric titration to determine their morphology, size and size distribution, zeta potential, and sulfate group density, respectively.

For TEM, NCs were characterized using high-resolution TEM instrument (JEM-2100, JEOL Ltd., Tokyo, Japan). NCs with a concentration of 0.003% (w/v) were prepared by diluting the stock suspension with DI water. The samples were stained with saturated uranyl acetate negative stain for high-resolution imaging.

The z-average hydrodynamic diameter (cumulant mean) and zeta potential of the NC nanoparticles were determined by DLS following the method described previously by Wang and Roman [26]. Measurements were performed in triplicate at 25°C using Brookhaven Instruments with Zeta Plus Particle Sizing Software (NanoBrook Omni, Brookhaven Instruments Corporation, USA). The samples were diluted in stock solution without adjustment of the pH or ionic strength.

Iron deficiency treatment of pear seedlings

P. betulifolia Bunge seeds were used as a plant material and stratified in river sand at a weight ratio of 1:10 and incubated in a refrigerator at 4°C for approximately 25 days. The germinated seeds were then planted in a soil matrix with a volume ratio of peat: perlite: vermiculite = 3:1:1 and grown in a greenhouse. When seedlings grew to 6–8 leaves, the seedlings were transferred to a hydroponic pot containing improved Hoagland's nutrient solution. The composition of the nutrient solution was 6 mM KNO_3, 4 mM $Ca(NO_3)_2{\cdot}4H_2O$, 2 mM KH_2PO_4, 1 mM $MgSO_4{\cdot}7H_2O$, 50 μM KCl, 25 μM H_3BO_3, 2 μM $MnSO_4{\cdot}H2O$, 2 μM $ZnSO_4{\cdot}7H_2O$, 0.5 μM $CuSO_4{\cdot}5H_2O$, 0.5 μM H_2MoO_4 (85% MoO_3) and 100 μM Fe(III)-EDTA. After one week, the plants were subjected to bicarbonate treatment (0.01 μM Fe(III)-EDTA, 2 mM $NaHCO_3$ and 0.5 g/L^{-1}, pH 7.2) for approximately one month to cultivate IDC pear seedlings, with three seedlings/pot and 15 min of ventilation per hour in the greenhouse [27].

When the plants grew to approximately 30 cm in height, the seedlings were moved to a growth chamber with 16 h of light (26°C) and 8 h of dark (18°C). After Fe deficiency treatment, the SPAD value of leaves was measured by a spad-502 portable chlorophyll analyzer. Leaves with SPAD values in the range of 10–30 were labeled for further measurement. The mean SPAD value of each pot was calculated from 20 leaves.

NCFe formulation, characterization, and treatments

NCFe was prepared by mixing NCs with ferrous sulfate solution based on the net charge density. Based on our pretests, three formulations of NCFe with charge density ratios of NCs to Fe of 1:300, 1:3000, and 1:30000 were prepared (Table 1). $FeSO_4$ and Fe-EDTA at the commonly used dose of 2 mmol/L was employed as positive controls, and DI water served as a negative control. In addition, 0.15% Tween-80 was supplemented to increase the adsorption capacity. The nanoparticles of NCFe were characterized using the same methods for NC characterization.

The treatments were performed by foliar application on the leaves of pear seedlings. During the operation, NCFe samples were freshly prepared by adding $FeSO_4$ to NCs before spraying. The three plants in each pot were evenly sprayed on the leaves with 8 mL of solution in total (Table 1). The final dose of Fe was 2 mmol/L in all treatments. The experiments were carried out in triplicate.

The root area was covered with plastic film to avoid the potential contamination of the nutrient solution with liquid from the leaves. When the liquid on the leaves dried, the treated plants were then transferred

into the growth chamber. The phenotype of the treated plants was observed, and related physiological indexes were determined after 72 h.

Table 1
Treatments with different formulations

Treatment*	Materials	NC:Fe (charge ratio)
Control	DI water	
T1	$FeSO_4$ + 0.15%TW**	
T2	NC + $FeSO_4$ + 0.15%TW	1:300
T3	NC + $FeSO_4$ + 0.15%TW	1:3,000
T4	NC + $FeSO_4$ + 0.15%TW	1:30,000
T5	Fe -EDTA + 0.15%TW	
* Each pot of 3 plants was sprayed with 8 mL of the solution.		
**TW, Tween 80.		

Physiological parameters and indicator measurements

The photosynthesis parameters in leaves, including net photosynthetic rate (Pn), stomatal conductance (Gs), intercellular CO_2 concentration (Ci), transpiration rate (Tr), saturated vapor pressure difference (VPD), and water use efficiency (WUE), were measured using a CIRAS-3 portable photosynthetic apparatus (PP Systems, Amesbury, MA 01913 USA).

The SPAD value was measured using a Spad-502 portable chlorophyll analyzer, and each leaf was measured three times. The middle part of the leaves was measured to avoid the midrib area. The total chlorophyll and carotenoids from leaves were extracted by 96% ethanol. A UV-Vis spectrophotometer (UV756, Youke Instrument, Shangahi, China) was used to determine the absorbance value of chloroplast pigment extract at 665 nm, 649 nm and 470 nm with 96% ethanol as a blank, and then the contents of chlorophyll a, chlorophyll b, total chlorophyll and carotenoid were calculated according to the method described by Wellburn and Lichtenthaler [28].

To determine the content of active Fe, the leaves were cut off from the plants without petioles. After washing, the leaves were dried at 105°C for 30 min followed by 70°C for one week in a DHG-9070A blast drying oven until reaching a constant weight. The measurement was conducted following the method described by Zhai et al [29]. Briefly, 100 mg of the dried leaves was crushed and extracted with 10 mL of 1.0 mol/L hydrochloric acid for 24 h under shaking. After filtration, the content of active Fe in the extraction solution was determined by a ZEEnit-700P atomic absorption spectrophotometer (Analytik Jena AG, Germany).

Analysis of active iron-related gene expression

For ferritin and PME extraction and analysis, leaf tissues were individually pulverized thoroughly with a mechanical grinding machine (KZ-III-FP, Servicebio, Wuhan, China) until a fine powder was obtained. Total RNA was extracted using an RNApure plant kit (CW0559, CWBio, Beijing, China) according to the manufacturer's instructions. RNA quality and quantity were checked by using a spectrophotometer (Nanodrop 2000, Thermo Fisher Scientific Inc., Wilmington, DE, USA). Single-stranded cDNA was synthesized using the ReverTra Ace® qPCR RT Kit (FSQ-101, TOYOBO, Shanghai, China) according to the manufacturer's instructions. Primer sequences were designed using the online software Primer3 (Table 2).

qRT-PCRs were performed on a TL988 real-time PCR system (TIANLONG, Xi'an, China) using 2X Universal SYBR Green Fast qPCR Mix (RK21203, Abclonal, Suzhou, China) with the following reaction conditions: 95°C denaturation for 5 min and 40 cycles of 5 s at 95°C and 34 s at 60°C, followed by melt curve stages to check that only single products were amplified. Every qRT-PCR was performed in biological triplicates, and *PbACTIN* was used as the reference gene for normalization of the templates. Expression profiles were analyzed using the ΔΔCT algorithm.

Table 2
PCR primers for the ferritin gene and pectin methylesterase gene

Target gene	Accession number	Primer sequences (5'–3')	Amplicon size (bp)
PbFER1	KM369967.1	Forward: GGCCATTTCGACGTTTTCC	133
		Reverse: TTTCGAGTTTTCGCTGCGG	
PbFER2	KM369968.1	Forward: GCGCTTCAAAGAACGCGAAT	84
		Reverse: CGAGGTCGAGCTCCTTCTTC	
PbFER3	KM369969.1	Forward: CTCTGAGGTCTGTTTCGGCA	82
		Reverse: GAGCTGAACAAGAGGGTGCT	
PbFER4	KM369970.1	Forward: TCCACTTGCACAGTGTTGCT	79
		Reverse: TGCTCGGTCAAATACTCGCT	
PbPME1	KC855753	Forward: AGGGTAGCTTCCCGACGTAT	133
		Reverse: GTATCGAGAGCAAAAGTGGCA	
PbPME3	KC855754	Forward: GCTTGCTTGGAGTGGAGACT	116
		Reverse: TGATCACATGGTAACCGGGC	
PbPME4	XM_009361399	Forward: CGAAAGCCGAGTCAAATGGC	99
		Reverse: AACCACAGGTCGCCTTCAAT	
PbACTIN	KT943411.1	Forward: CTTCCCGATGGCCAAGTCAT	103
		Reverse: CATGAATGCCAGCAGCTTCC	

Statistical analysis

The results are presented as the mean ± standard deviation (SD). IBM SPSS version 22 was used for statistical analyses. Significance of means was assessed using analyses of variance (ANOVA), and Duncan's multiple range test was implemented to compare means at the $p = 0.05$ level of significance. Each treatment was carried out in triplicate.

Results And Discussion

Physicochemical properties of NC and NCFe

The morphologies of NC and NCFe particles were visualized by TEM. The morphology of the NC particles was that of rod-like whiskers (Fig. 1a), which was in agreement with previous reports on NCs [26, 30]. When NCs were mixed with $FeSO_4$, the NCFe particles maintained a small, whisker-like morphology with small dots (Fe) on the surface of the NC particles (Fig. 1b). The Z-average hydrodynamic diameter and

zeta potential of the NC whiskers measured by DLS were 84.3 ± 0.2 nm and − 47.3 ± 1.7 mV (Fig. 2b), respectively, with a polydispersity index (PDI) of 0.20 ± 0.01 (Fig. 2a). The particle size and zeta potential of NC-Fe were 107.4 ± 3.0 nm and − 9.7 ± 0.4 mV, respectively, with a PDI of 0.36 ± 0.05 (Fig. 2c and 2d).

NC synthesis includes partial esterification using sulfuric acid under appropriate conditions [26]. Hence, sulfonic groups on the surface of NCs can be determined by means of conductometric titration, which was developed by several groups in 1925 [31, 32]. Figure 3 shows a typical V-shaped titration curve of the conductivity of the NCs. The net charge density calculated by the consumption of titrant for sulfate group neutralization was 112 ± 6.4 mmol/kg in this study.

The surface chemistry of charged nanoparticles significantly affects their biological performance. The net charge density of NCs in aqueous suspension is an important parameter to measure biological activity. A well-dispersed suspension can be easily applied on the plant surface by the spraying method. The size and size distribution of a charged nanomaterial in aqueous solution greatly affect the efficiency of spraying. A negative zeta potential value indicates that the nanoparticle was negatively charged. The net charge density of the NCs indicated the magnitude of ionizable groups on the surface of the particles. A higher net charge density or zeta potential of nanoparticles supplies a stronger repel force to suspend particles in solution, providing a great opportunity to chelate Fe ions for the transportation and dispersion of Fe into a biological system or pectin in the plant cell wall [13].

Phenotype of pear leaves treated with NCFe

Figure 4 shows the phenotypic comparison of pear seedlings grown under the Fe deficiency treatments or normal hydroponic culture. Under low - Fe concentrations, the leaves showed visible symptoms of chlorosis (Fig. 4a). When using Hoagland's nutrient solution containing 1×10^{-4} mol/L Fe-EDTA, the seedlings grew well without obvious chlorosis (Fig. 4b). However, as shown in Fig. 4c, after 72 h of treatment with NCFe (T2-T4) and Fe-EDTA (T5), more evenly distributed green color appeared in the leaves, but ferrous sulfate (T1)-treated leaves were only partially recovered with uneven distribution of a green color, and the yellow leaves still showed green spots. Thus, increased Fe uptake was observed in the NCFe treatments.

The rod-like particles of NCs with a negative zeta potential indicated that the particles were negatively charged (Fig. 2b). It has been proven that NCs have a higher adsorption capacity and better binding affinity than other similar materials at the macroscale [22]. When NCs are mixed with Fe^{2+}, the high content of available sulfonic groups on the NC surfaces is utilized as an anchor point for the simultaneous reduction and stabilization of NC-supported Fe^{2+}. The use of NCs as carriers to restore the availability of Fe could be a valuable and sustainable strategy to reduce the impact of Fe chlorosis on pear and/or crops [33]. This phenomenon may be attributed to the increased interaction between the positively charged metal salt and negatively charged NCs due to the presence of sulfonic groups on the NC surface and iron chelating properties [34, 35].

Fe ions bound to anionic NC whiskers could increase Fe transportation capability and promote active Fe migration to Fe-deficient plants. The phenotype of pear leaves treated with NCFe indicated that in the leaves sprayed with ferrous sulfate alone (Fig. 4c, T1), ferrous ions may not be efficiently absorbed or evenly transported to other places. In the leaves treated with NCFe (Fig. 4c, T2-T4), depending on the formulation of NCs to Fe, ferrous ions could be easily transported into plant cells and increase the active Fe and chlorophyll contents in the cell to improve the photosynthetic rate. We therefore assumed that NCs performed as carriers to bring ferrous ions into leaves and distribute evenly; hence, the leaves returned to green more sufficiently. Comparably, the greenness of the Fe-EDTA-treated plants (Fig. 4c, T5) was between those of the ferrous sulfate- and NCFe-treated plants, indicating that the level of re-greening might be dependent on foliar fertilizer formulation and/or facilitators.

However, a relatively high Fe concentration was not necessarily correlated with re-greening rates because the effectiveness and mobilization of Fe may be restricted within the leaf [36]. We observed that NCFe prepared at a charge ratio of 1:3000 was an optimal formulation to control chlorosis. This finding also agreed with a previous report performed by Fernández et al [37]. The release dynamics and metabolic mechanism of NCFe within Fe-deficient plants at the molecular level should be further explored in the future.

Enhancement of the photosynthetic rate of pear leaves

To study the impacts of NCFe on photosynthesis, we mainly explored the effects of NCFe with an optimal NC-to-Fe ratio (T3) and compared them to those of ferric sulfate (T1) on photosynthetic parameters, including the Pn of leaves, Gs, Ci, Tr, VPD, and WUE. As shown in Table 3, the Pn of T1 and T3 was significantly increased by the NCFe treatment compared with that of CK, and the Pn of T3 was 121.7% higher than that of CK and 40.4% higher than that of T1. In addition, the Gs, Tr and WUE of T3 were significantly increased compared with those of the CK, and there were no significant differences in these parameters between the T1 and CK groups. The Ci and VPD of the CK group were higher than those of the T1 and T3 groups, and there was a significant difference in these parameters between T3 and CK but not between T3 and T1.

Photosynthesis is a complex comprehensive photochemical and biochemical process that is not only light-dependent and takes place in the thylakoidal membrane of chloroplasts but also occurs in the stroma of chloroplast fixation, reduction of CO_2 and formation of carbohydrates [38]. It has been reported that metallic nanoparticles and oxides can be used as photocatalysts to convert light to energy and promote the photosynthetic rate when associated with the structure and function of plant photosynthesis [39]. However, preventing and controlling iron chlorosis is difficult and often gives poor results, but copper-iron chelation, for example, could enhance the photosynthetic rate in IDC grape leaves [40]. Our results also demonstrated that spraying NCFe could significantly improve the photosynthetic capacity and photosynthetic rate of leaves compared with the treatment of spraying $FeSO_4$.

Table 3
Effects of treatments on the photosynthetic parameters of pear leaves

Treatment*	Pn*	Gs	Ci	Tr	VPD	WUE
CK	6.9 ± 0.8 c	236 ± 23.7 b	341.3 ± 8.0 b	4.9 ± 0.3 b	2.1 ± 0.1 b	1.4 ± 0.2 b
T1	10.9 ± 0.4 b	328.3 ± 13.2 ab	330.7 ± 2.6 ab	5.9 ± 0.1 a	1.9 ± 0.1 a	1.8 ± 0.1 b
T3	15.3 ± 1.8 a	428.0 ± 49.1 a	319.0 ± 6.7 a	5.8 ± 0.1 a	1.5 ± 0.1 a	2.7 ± 0.3 a

*T1, 2 mmol/L $FeSO_4$; T3: chelate prepared at a NC-to-Fe charge ratio of 1:3000. Pn, net photosynthetic rate of leaves; Gs, stomatal conductance; Ci, intercellular CO_2 concentration; Tr, transpiration rate; VPD, saturated vapor pressure difference; and WUE, water use efficiency.

Enrichment of physiological indicators facilitated by NCFe

Chlorophyll content, active Fe content, and chlorophyll fluorescence parameters are major physiological indicators for studying plant physiological processes [41]. In this study, the SPAD value was used to evaluate the effects of NCFe on the chlorophyll content in leaves (Fig. 5). The results showed that after 72 h of treatment, the chlorophyll content increased from high to low in the following order: T3 > T4 > T2 > T5 > T1 > CK. The chlorophyll content enhancement in treatments T2 to T5 was significantly higher than that in T1 and the control. However, there was no significant difference ($p < 0.05$) among the NCFe treatments from T2 to T4.

Table 4
Chlorophyll and carotenoid contents of leaves after 72 h of treatment

Treatment*	SPAD	Chlorophyll a	Chlorophyll b	Total Chlorophyll	Carotenoid
CK	21.6 ± 1.2 c	0.40 ± 0.003 c	0.12 ± 0.003 c	0.52 ± 0.005 c	0.19 ± 0.007 b
T1	30.1 ± 1.3 b	0.61 ± 0.034 b	0.16 ± 0.013 b	0.78 ± 0.025 b	0.22 ± 0.019 b
T3	37.3 ± 1.0 a	0.85 ± 0.096 a	0.26 ± 0.029 a	1.11 ± 0.130 a	0.32 ± 0.033 a

*T1, 2 mmol/L $FeSO_4$; T3: chelate prepared with a NC-to-Fe charge ratio of 1:3000. All suspensions were diluted with DI water. Means followed by different letters present significant differences at $p < 0.05$.

Table 4 showed that the contents of chlorophyll a, chlorophyll b and total chlorophyll of T1 and T3 were significantly increased compared with those of CK, and the contents of chlorophyll a, chlorophyll b and total chlorophyll of T3 treatment were significantly higher than those of T1, which were increased by 112.5%, 116.7%, and 113.5% compared with the CK and 39.3%, 62.5%, and 42.3% compared with T1, respectively. The carotenoid content in the leaves of T3 was significantly increased compared with that of T1 and CK, but there was no significant difference in the carotenoid content between T1 and CK. The

results showed that the chlorophyll and carotenoid contents of plants were increased significantly by spraying NCFe compared with those of plants sprayed $FeSO_4$.

The effects of NCFe on the active Fe content in seedling leaves are shown in Fig. 6. After 72 h of treatment, the active iron contents in the T1 to T5 treatments were all significantly increased compared with that of the control. More importantly, the active iron content in the NCFe treatments (T2, T3, and T4) was much higher than that of the $FeSO_4$ (T1) and Fe-EDTA (T5) treatments. In particular, when the chelate prepared with a NC-to-Fe charge ratio of 1:3000 (T3) was applied, the active Fe content of the treated leaves was significantly enhanced compared with all other treatments. More specifically, the active Fe content increased approximately 9 times compared with that of the control. The results demonstrated that NCs had a strong ability to promote the active Fe content in the leaves, so the IDC of pear leaves was obviously controlled and eventually reversed.

Chlorophyll and carotenoids are major light-harvesting pigments. The value of chlorophyll fluorescence describes plant photosynthetic growth and mechanisms. The light energy absorbed by chlorophyll is mainly consumed by photosynthesis, chlorophyll fluorescence and heat dissipation [42]. This study showed that NCFe could increase the chlorophyll contents up to more than 70% compared with the control (Table 4) and strongly promoted chlorophyll fluorescence parameters in IDC leaves (Table S1). A previous study showed that sulfate group density played an important role in the chelation of Fe to NCs and/or in their biological activity [43]. Our results indicated that different concentrations of NCs in the NCFe formulation had different impacts on chlorosis recovery (Fig. 4c). At an appropriate chelation formulation, CNFs could enhance physiological indicators (Fig. 5) and even increase the chlorophyll contents up to more than 70% compared with the control (Table 4). A small increase in chlorophyll and carotenoids comes together to form a reaction center where the absorbed light energy is initially converted into chemical energy, resulting in plant healthy growth [12].

Regulation of relative gene expression in pear leaves

Ferritin plays an important role in iron storage in plants [11]. We mainly studied the relative expression levels of *P. betulifolia* ferritin genes (*PbFER1*, *PbFER2*, *PbFER3* and *PbFER4*) in leaves as well as PME gene expression. The results showed that expression levels of ferritin genes *PbFER1*, *PbFER2* and *PbFER3* in the T1 and T3 plants were significantly upregulated compared to those in CK plants after 72 h of treatment, and the relative expression levels of the three genes in the T3 plants were significantly higher than those in the T1 plants (Fig. 7). The expression levels of *PbFER1*, *PbFER2* and *PbFER3* in T3 plants were 3.6, 4.2 and 4.0 times those in CK plants and 1.5, 1.6 and 1.7 times those in T1 plants, respectively. The relative expression level of *PbFER4* in T3 was significantly higher than that in T1 and CK, but there was no significant difference between T1 and CK. The relative expression levels of *PbFER1*, *PbFER2*, *PbFER3* and *PbFER4* in leaves were generally higher than those in roots, stems and fruits [11]. As reported by Santos et al. [44], spraying [Fe(MPP)3] iron fertilizer increased ferritin gene expression 2-fold, and the chlorophyll content and active iron content of soybean leaves were significantly increased by 29% and 36%, respectively. The results of this study indicated that spraying NCFe on IDC leaves could

effectively improve the relative expression of the ferritin gene in leaves and then increase the active iron content in leaves.

The results of NCFe-regulated PME gene expression are shown in Fig. 8. After 72 h of treatment, the PME gene expression levels of *PbPME1, PbPME3*, and *PbPME4* in CK plants were significantly higher than those in T1 and T3 plants, and the relative expression levels of *PbPME1* and *PbPME4* in T1 plants were significantly higher than those in T3 plants. However, there was no significant difference in the relative expression of *PbPME3* between T1 and T3 plants. The relative expression levels of *PbPME1, PbPME3*, and *PbPME4* in CK plants were 2.7, 1.8, and 7.3 times those in T3 plants and 1.4, 1.8, and 1.7 times those in T1 plants, respectively. The results showed that compared with that in CK and T1 plants, the relative expression of *PbPME1* and *PbPME4* in plants sprayed with NCFe decreased the most, indicating that pectin will be in a more methylated form and not bind to iron.

Pectin is one of the main components of the cell wall [45] and is usually secreted from the Golgi apparatus into the cell wall in highly methylated forms [46] and then undergoes demethylation by PME, consequently increasing metal ion binding sites in the cell wall [47]. On the other hand, soil bicarbonate can increase the apoplast pH of leaves, and the activity of PME increases as the pH increases, thereby enhancing iron precipitation in the apoplast and reducing its bioavailability [48, 49]. In this study, NCFe could significantly reduce the expression of *PbPME* due to sulfonic acid groups on NCFe and effectively reduce the apoplast pH. A relatively PME activity further reduces the precipitation of iron in the apoplast and improves its bioavailability.

Overall, to prevent Fe chlorosis, the application of synthetic Fe chelates is a common practice to increase the solubility of Fe and function as a transporter through solution to the plant [50]. However, the efficiency of foliar fertilization in pear Fe deficiency disease control was not significant as expected [10]. It is possible that leaf structure significantly affects the efficiency of Fe penetration and relocation when ferrous sulfate is sprayed on pear leaves [6, 8]. Nevertheless, the ferrous sulfate only acted on the adherent part, new leaves were still yellow because Fe was quickly fixed, and green spotting was still shown on the leaves [51]. Here, our results showed even re-greening in Fe-deficient leaves after NCFe treatment. This demonstrated that NCFe facilitated photosynthesis by stimulating the absorption of Fe in Fe-deficient leaves. The simplest possible mechanism to make Fe available is through inducing ferritin gene expression to express more ferritin for iron storage, down regulating PME gene expression and decreasing the binding affinity to iron on the cell wall but increasing the active Fe content in leaves. NCs had a strong ability to improve the dispersibility of active Fe when NCFe was applied in situ.

Conclusion

This is the first report of whisker-like NC application in plant IDC control. We demonstrated that NCs have strong potential to promote plant photosynthesis, which is attributed to the enhancement of photosynthesis parameters and indicators. NCFe treatment significantly downregulated the expression of the PME gene (*PbPME*) and upregulated the expression of the ferritin gene (*PbFER*) to increase the active

iron content. The possible photosynthetic mechanism might attribute to the enhancements of C_{Fe}, Pn, Gs, Ci, Tr, VPD, and WUE as well as the regulation of relative genes expression. This finding will provide a good alternative and a complementary strategy for Fe-chelate applications in plant iron chlorosis management.

Declarations

Acknowledgements

The authors thank those who provided help to our experiments in both Institute of Horticulture, Henan Academy of Agricultural Sciences and Colleges of Plant Protection at Henan Agricultural University. The first and second authors contributed equally to this study.

Authors' contributions

XG and HW conceived and designed the experiments. YB, and QQ performed the experiments. XG, YB analyzed the data and wrote the manuscript. ZL and ZW provided technical support for plant growth. QW and BZ provided technical support for the preparation and characterization of nanocrystal cellulose, nanocellulose-iron chelation. HW and DW reviewed and edited the manuscript. All authors read and approved the final manuscript.

Funding

This study was supported by Scientific and technological research in Henan Province (21210211412); China Agriculture Research System of MOF and MARA; Special Fund for Research and Development, Henan Academy of Agricultural Sciences (20188106) and National Key Research and Development Program, Ministry of Science and Technology of People's Republic of China (2018YFD0201400).

Ethics approval and consent to participate

Not applicable.

Consent for publication

Not applicable.

Competing interests

The authors declare that they have no competing interests.

Author details

1 Institute of Horticulture, Henan Academy of Agricultural Sciences, Zhengzhou, 450002, China. 2 College of Plant Protection, Henan Agricultural University, Zhengzhou 450002, China. 3 NanoAgro Center, Henan

Agricultural University, Zhengzhou 450002, China.

References

1. Chapman GW. The relation of iron and manganese to chlorosis in plants. New Phytol. 1931;30:266–83.
2. Thomasraese J, Staiff D. Chlorosis of 'Anjou' pear trees reduced with foliar sprays of iron compounds. J Plant Nutri. 1988;11:1379–85.
3. He T, Liu Z, Qin W, Tian Y, Zhang S. **Effects of soil factors on iron-deficit chlorosis of Kuerle Fragrant Pear (***Pyrus Bretschneideri* **Rehd)** *Acta Agri Boreali-Occident Sin* 2013, 22:97–103 (in Chinese with English abstract).
4. El-Deen E, Attia MF, Sheren EH. Response of Pear (Le Conte cv.) Trees Grown in Calcareous Soil to Trunk Injection and Foliar Application of some Micronutrients. Alexandria Sci Exchange J. 2018;39:747–61.
5. Ikinci A, Bolat I, Ercisli S, Esitken A. Response of yield, growth and iron deficiency chlorosis of "Santa Maria" pear trees on four rootstocks. Not Bot Horti Agrobot. 2016;44:563–7.
6. Fernández V, Eichert T, Del Río V, López-Casado G, Heredia-Guerrero JA, Abadía A, Heredia A, Abadía J. Leaf structural changes associated with iron deficiency chlorosis in field-grown pear and peach: physiological implications. Plant Soil. 2008;311:161–72.
7. Álvarez-Fernández A, Melgar JC, Abadía J, Abadía A. **Effects of moderate and severe iron deficiency chlorosis on fruit yield, appearance and composition in pear** *(Pyrus communis* **L.) and peach (***Prunus persica* **(L.) Batsch)**. Environ Exp Bot. 2011;71:280–6.
8. El-Dahshouri MF, Hamouda HA, Hafez OM, Khafagy SA: **Enhancing le-conte pear trees performance by foliar spray with different Iron concentrations** *Agric Eng Int* 2017, **Special Issue**:201–210.
9. Yuan Z, Vanbriesen JM. The Formation of Intermediates in EDTA and NT A Biodegradation. Environ Eng Sci. 2006;23:533–44.
10. Álvarez-Fernández A, García-Laviña P, Fidalgo C, Abadía J, Abadía A. **Foliar fertilization to control iron chlorosis in pear (***Pyrus communis* **L.) trees**. Plant Soil. 2004;263:5–15.
11. Xi L, Xu K, Qiao Y, Qu S, Zhang Z, Dai W. Differential expression of ferritin genes in response to abiotic stresses and hormones in pear (Pyrus pyrifolia). Mol Biol Rep. 2011;38:4405–13.
12. Hashimoto H, Uragami C, Cogdell RJ: **Carotenoids and photosynthesis**. In *Carotenoids in Nature: Biosynthesis, Regulation and Function.* Edited by Stange C. Cham: Springer International Publishing; 2016: 111–139.
13. Chaichi M, Hashemi M, Badii F, Mohammadi A. Preparation and characterization of a novel bionanocomposite edible film based on pectin and crystalline nanocellulose. Carbohydr Polym. 2017;157:167–75.
14. Jolie RP, Duvetter T, Van Loey AM, Hendrickx ME. Pectin methylesterase and its proteinaceous inhibitor: a review. Carbohydr Res. 2010;345:2583–95.

15. Fernández V, Ebert G. Foliar iron fertilization: A critical review. J Plant Nutr. 2005;28:2113–24.
16. Malhotra H, Pandey R, Sharma S, Bindraban PS. Foliar fertilization: possible routes of iron transport from leaf surface to cell organelles. Arch Agron Soil Sci. 2020;66:279–300.
17. Chhipa H. Nanofertilizers and nanopesticides for agriculture. Environ Chem Lett. 2017;15:15–22.
18. Khan MR, Rizvi TF: **Application of nanofertilizer and nanopesticides for improvements in crop production and protection**. In *Nanoscience and Plant–Soil Systems.* Edited by Ghorbanpour M, Manika K, Varma A. Cham: Springer International Publishing; 2017: 405–427.
19. Song Y, Zhou Y, Chen L. Wood cellulose-based polyelectrolyte complex nanoparticles as protein carriers. J Mater Chem. 2012;22:2512–9.
20. Shen X, Shamshina JL, Berton P, Gurau G, Rogers RD. Hydrogels based on cellulose and chitin: fabrication, properties, and applications. Green Chem. 2016;18:53–75.
21. Bossa N, Carpenter AW, Kumar N, de Lannoy C-F, Wiesner M. Cellulose nanocrystal zero-valent iron nanocomposites for groundwater remediation. Environ Sci Nano. 2017;4:1294–303.
22. Faiz Norrrahim MN, Mohd Kasim NA, Knight VF, Mohamad Misenan MS, Janudin N, Ahmad Shah NA, Kasim N, Wan Yusoff WY, Mohd Noor SA, Jamal SH, et al. Nanocellulose: a bioadsorbent for chemical contaminant remediation. RSC Adv. 2021;11:7347–68.
23. Mat Zaid MH, Che-Engku-Chik CEN, Yusof NA, Abdullah J, Othman SS, Issa R, Md Noh MF, Wasoh H. **DNA electrochemical biosensor based on iron oxide/nanocellulose crystalline composite modified screen-Printed carbon electrode for detection of** *Mycobacterium tuberculosis*. Molecules. 2020;25:3373.
24. Baruah J, Chaliha C, Kalita E, Nath B, Field R, Deb P. Modelling and optimization of factors influencing adsorptive performance of agrowaste-derived nanocellulose iron oxide nanobiocomposites during remediation of arsenic contaminated groundwater. Int J Biol Macromol. 2020;164:53–65.
25. Dong S, Bortner MJ, Roman M. Analysis of the sulfuric acid hydrolysis of wood pulp for cellulose nanocrystal production: A central composite design study. Ind Crops Prod. 2016;93:76–87.
26. Wang H, Roman M. Formation and properties of chitosan – cellulose nanocrystal polyelectrolyte – Macroion complexes for drug delivery applications. Biomacromol. 2011;12:1585–93.
27. Guo X, Wu Z, Wang D, Zhang S, Niu J. **Bioinformatics analysis of iron uptake key gene in the root of** *Pyrus betulifolia* **and the effect of iron deficiency on its expression**. J Henan Agric Sci. 2017;46:96–101. (in Chinese with English abstract).
28. Wellburn AR, Lichtenthaler H: **Formulae and Program to Determine Total Carotenoids and Chlorophylls A and B of Leaf Extracts in Different Solvents**. In *Advances in Photosynthesis Research, Advances in Agricultural Biotechnology. Volume* 2. Edited by Sybesma C. Dordrecht: Springer,; 1984: 9–12.
29. Zhai L, Xiao D, Sun C, Wu T, Han Z, Zhang X, Xu X, Wang Y. **Nitric oxide signaling is involved in the response to iron deficiency in the woody plant** *Malus xiaojinensis*. Plant Physiol Biochem. 2016;109:515–24.

30. Beck-Candanedo S, Roman M, Gray DG. Effect of reaction conditions on the properties and behavior of wood cellulose nanocrystal suspensions. Biomacromol. 2005;6:1048–54.
31. Raurich Sas FE. Determination of morphine by conductometric titration with silicotungstic acid. J Chem Soc Abstr. 1925;128:ii998–1012.
32. Usher FL. The nature of the interfacial layer between an aqueous and a non-aqueous phase. Trans Faraday Soc. 1925;21:406–24.
33. Baldi E, Marino G, Toselli M, Marzadori C, Ciavatta C, Tavoni M, Di Giosia M, Calvaresi M, Falini G, Zerbetto F. Delivery systems for agriculture: Fe-EDDHSA/CaCO3 hybrid crystals as adjuvants for prevention of iron chlorosis. Chem Commun. 2018;54:1635–8.
34. Kang E, Je HH, Moon E, Na J-G, Kim MS, Hwang DS, Choi YS. **Cellulose nanocrystals coated with a tannic acid-Fe^{3+} complex as a significant medium for efficient CH_4 microbial biotransformation**. Carbohydr Polym. 2021;258:117733.
35. Dhar P, Kumar A, Katiyar V. Fabrication of cellulose nanocrystal supported stable Fe(0) nanoparticles: a sustainable catalyst for dye reduction, organic conversion and chemo-magnetic propulsion. Cellulose. 2015;22:3755–71.
36. El-Jendoubi H, Vázquez S, Calatayud A, Vavpetič P, Vogel-Mikuš K, Pelicon P, Abadía J, Abadía A, Morales F: **The effects of foliar fertilization with iron sulfate in chlorotic leaves are limited to the treated area**. **A study with peach trees** (Prunus persica **L. Batsch**) **grown in the field and sugar beet** (Beta vulgaris **L.**) **grown in hydroponics**. *Front Plant Sci* 2014, **5**:Article 2.
37. Fernández V, Del Río V, Pumariño L, Igartua E, Abadía J, Abadía A. **Foliar fertilization of peach (***Prunus persica* **(L.) Batsch) with different iron formulations: Effects on re-greening, iron concentration and mineral composition in treated and untreated leaf surfaces**. Sci Hortic. 2008;117:241–8.
38. Tighe-Neira R, Carmora E, Recio G, Nunes-Nesi A, Reyes-Diaz M, Alberdi M, Rengel Z, Inostroza-Blancheteau C. Metallic nanoparticles influence the structure and function of the photosynthetic apparatus in plants. Plant Physiol Biochem. 2018;130:408–17.
39. Liu L, Zhang X, Yang L, Ren L, Wang D, Ye J. Metal nanoparticles induced photocatalysis. Natl Sci Rev. 2017;4:761–80.
40. Ma J, Zhang M, Liu Z, Chen H, Li YC, Sun Y, Ma Q, Zhao C. **Effects of foliar application of the mixture of copper and chelated iron on the yield, quality, photosynthesis, and microelement concentration of table grape (***Vitis vinifera* **L.)**. Sci Hortic. 2019;254:106–15.
41. Fan XY, Liu WY, Song L, Liu S, Shi XM, Yuan GD. A combination of morphological and photosynthetic functional traits maintains the vertical distribution of bryophytes in a subtropical cloud forest. Am J Bot. 2020;107:761–72.
42. Tokarz K, Makowski W, Banasiuk R, Krolicka A, Piwowarczyk B. **Response of** *Dionaea muscipula* **J. Ellis to light stress in** *in vitro*: **physiological study**. Plant Cell Tissue Organ Cult. 2018;134:65–77.
43. Jiang F, Kittle JD, Tan X, Esker AR, Roman M. Effects of Sulfate Groups on the Adsorption and Activity of Cellulases on Cellulose Substrates. Langmuir. 2013;29:3280–91.

44. Santos CS, Rodrigues E, Ferreira S, Moniz T, Leite A, Carvalho SM, Vasconcelos MW, Rangel M. Foliar application of 3-hydroxy-4-pyridinone Fe-chelate [Fe (mpp) 3] induces responses at the root level amending iron deficiency chlorosis in soybean. Physiol Plant. 2021;173:235–45.
45. Cosgrove DJ. Growth of the plant cell wall. Nat Rev Mol Cell Biol. 2005;6:850–61.
46. Gaffe J, Morvan C, Jauneau A, Demarty M. Partial purification of flax cell wall pectin methylesterase. Phytochemistry. 1992;31:761–5.
47. Zhang Z, Wang H, Wang X, Bi Y. Nitric oxide enhances aluminum tolerance by affecting cell wall polysaccharides in rice roots. Plant Cell Rep. 2011;30:1701–11.
48. Mengel K, Planker R, Hoffmann B. **Relationship between leaf apoplast pH and iron chlorosis of sunflower (***Helianthus annuus* **L.)**. J Plant Nutr. 1994;17:1053–65.
49. Del Corpo D, Fullone MR, Miele R, Lafond M, Pontiggia D, Grisel S, Kieffer-Jaquinod S, Giardina T, Bellincampi D, Lionetti V. **AtPME17 is a functional** *Arabidopsis thaliana* **pectin methylesterase regulated by its PRO region that triggers PME activity in the resistance to** *Botrytis cinerea*. Mol Plant Pathol. 2020;21:1620–33.
50. Schenkeveld WDC, Temminghoff EJM, Reichwein AM, van Riemsdijk WH. FeEDDHA-facilitated Fe uptake in relation to the behaviour of FeEDDHA components in the soil-plant system as a function of time and dosage. Plant Soil. 2010;332:69–85.
51. Zou C, Chen X, Zhang F, Mao D. Study on the correlation between the active Fe and Fe nutritional status of plan. J Plant Nutr Fert (in Chinese with English abstract). 1998;1998:399–406.

Figures

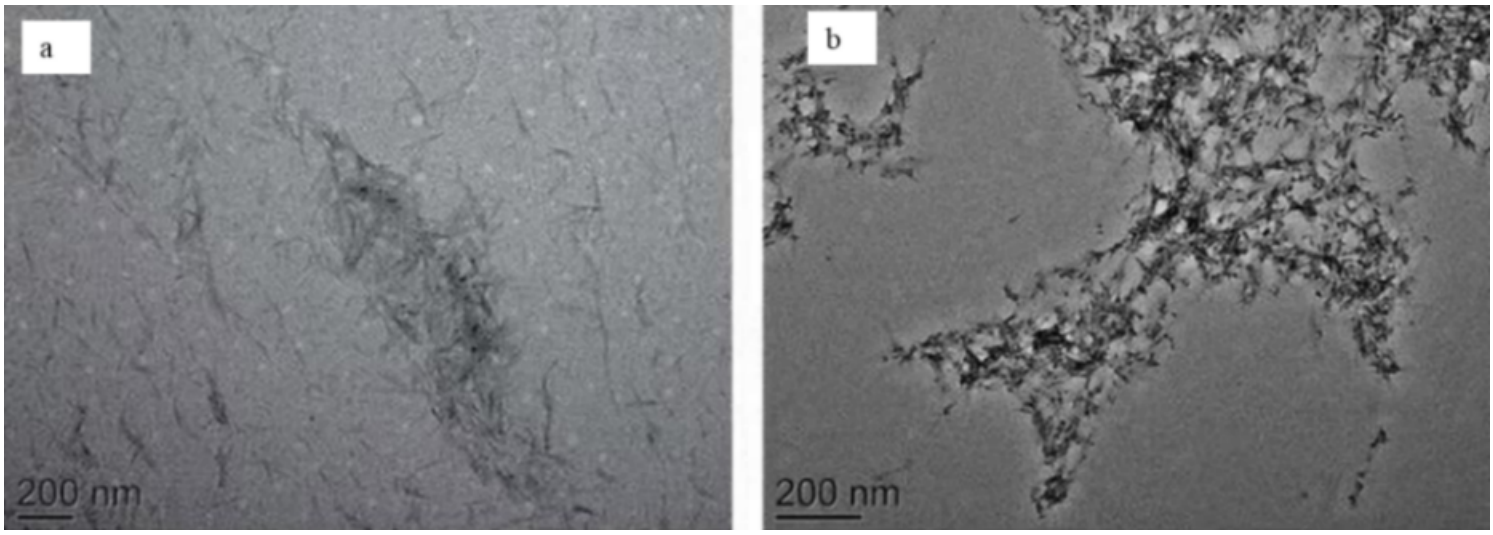

Figure 1

TEM images of NCs and NCFe. a) A solution of 0.03% (w/v) NCs were prepared by diluting the stock suspension with DI water; b) 0.03% w/v NCFe.

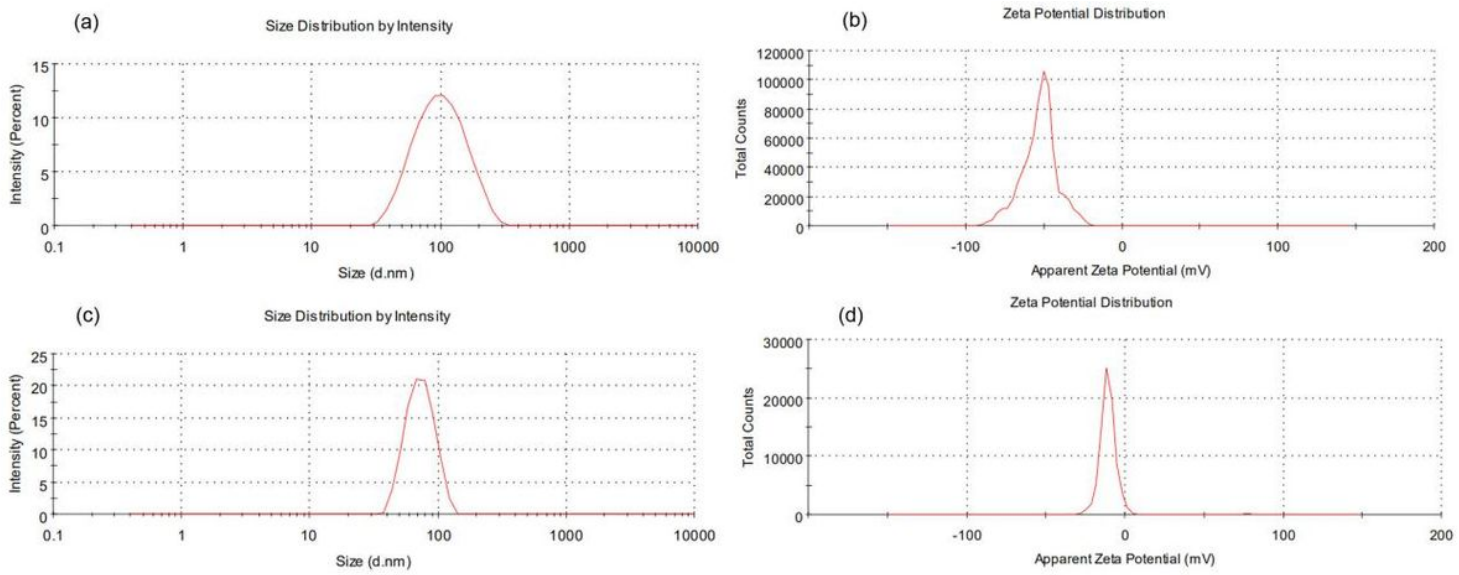

Figure 2

Particle size and zeta potential of NCs and NCFe measured by DLS. (a) The size and size distribution of NCs (0.03% wt/v). (b) Zeta potential of the NC suspension. (c) The size and size distribution of NCFe formulated at a charge density ratio of 1:3000. (d) Zeta potential of NCFe with same formulation.

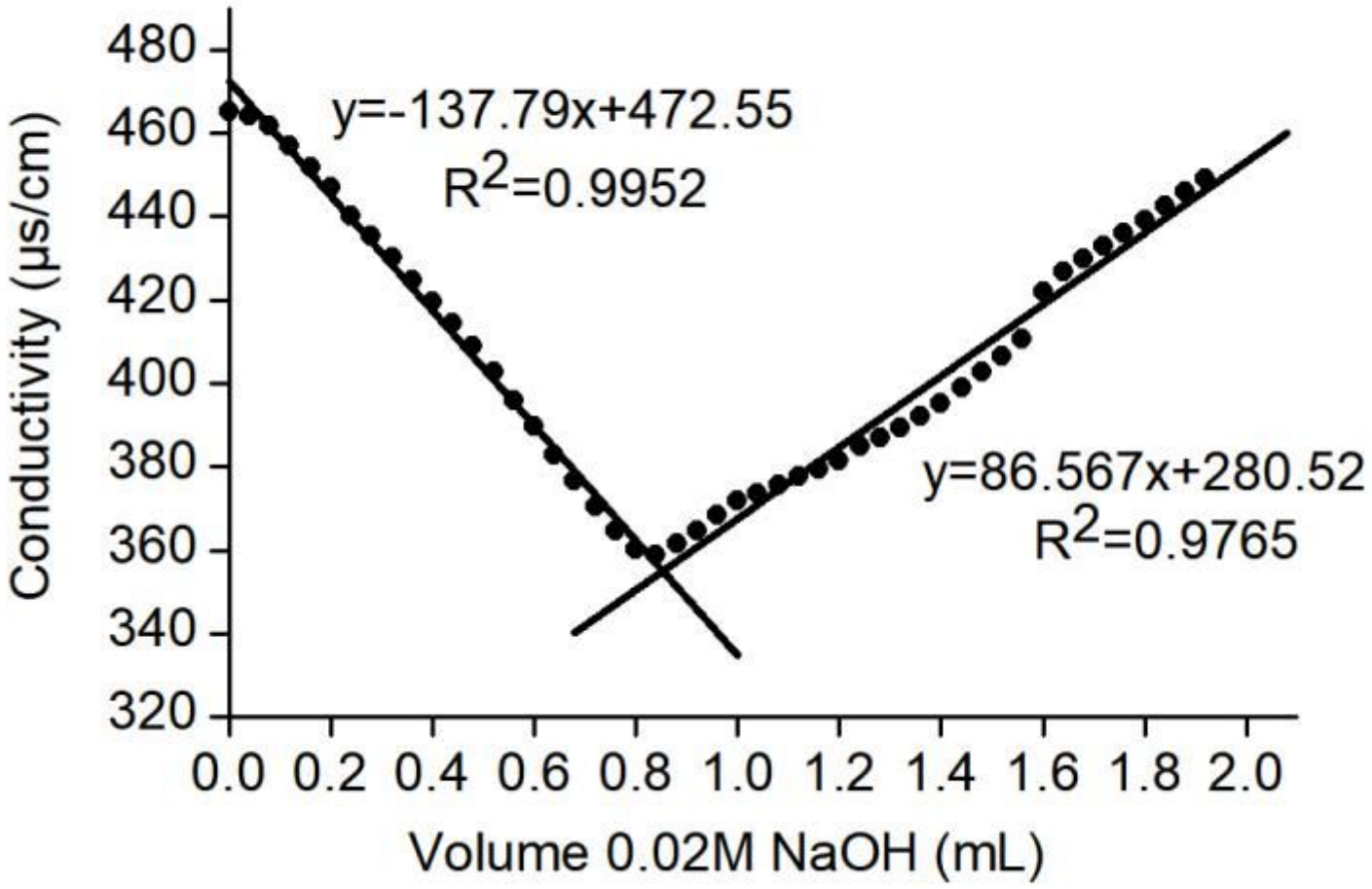

Figure 3

Conductometric titration curves of the NCs. Approximately 25 mL of stock suspension of NCs was titrated with 0.02 M NaOH. The ionic strength of the solution was adjusted to 0.01 mM with NaCl. The results were the means of three measurements.

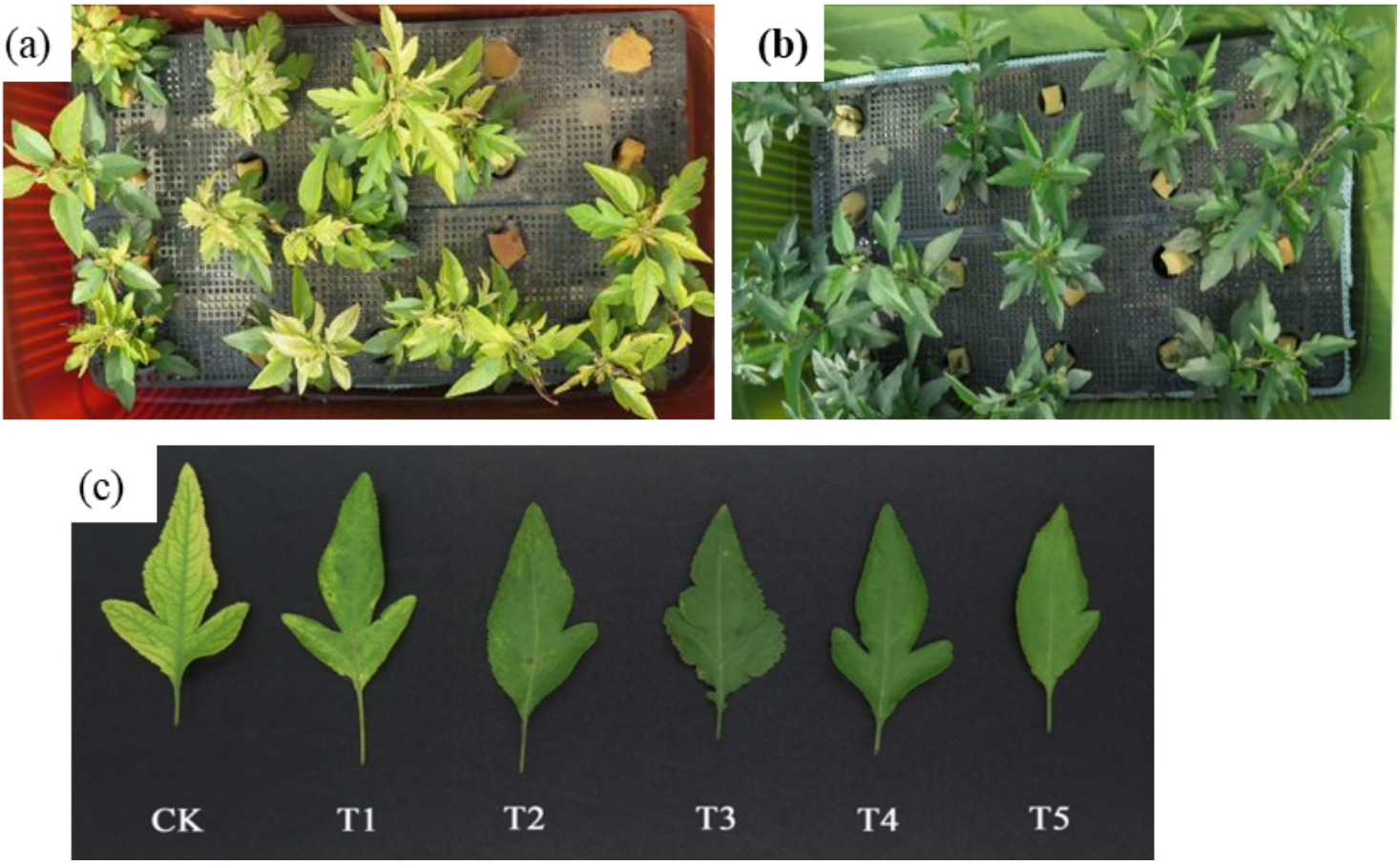

Figure 4

Phenotypic comparison of pear seedlings between treatments and normal hydroponic cultures. (a) Fe deficiency plants treated with Hoagland's nutrient solution containing 1×10-8 mol/L Fe-EDTA. (b) Plants treated with Hoagland's nutrient solution containing 1×10-4 mol/L Fe-EDTA. (c) Phenotypes of pear seedling leaves under different treatments. CK: DI water; T1: 2 mmol/L FeSO4; T2-T4: chelate obtained with a NC-to-Fe charge ratio of 1:300, 1:3000; and 1:30000, respectively; T5: 2 mmol/L Fe-EDTA. The final concentration of Fe in the chelates was 2 mmol/L FeSO4.

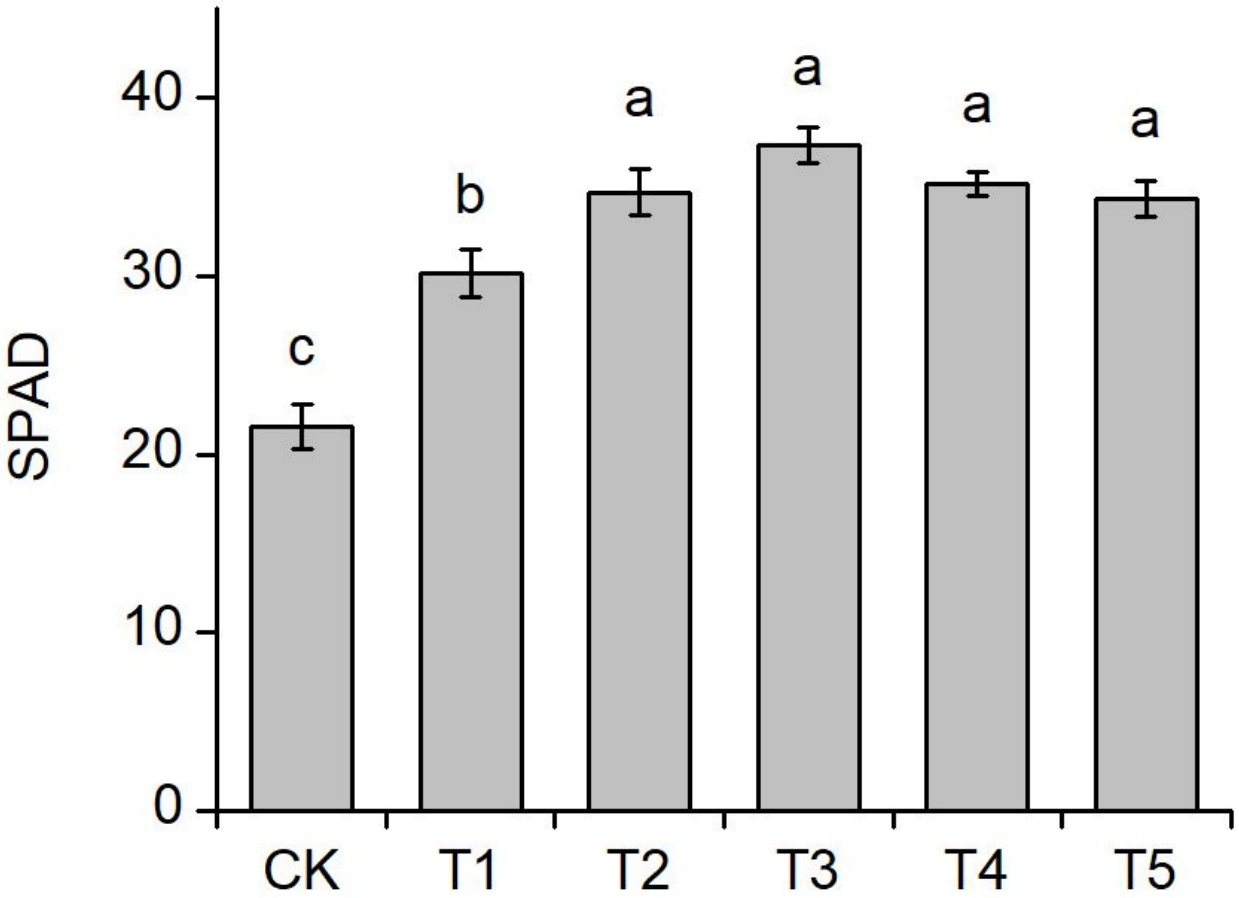

Figure 5

Chlorophyll contents of leaves after 72 h. T1: 2 mmol/L FeSO4; T2-T4: chelates prepared with a NC-to-Fe charge ratio of 1:300, 1:3000, and 1:30000, respectively; T5: 2 mmol/L Fe-EDTA; CK: DI water. All suspensions were diluted with DI water. Means followed by different letters present significant differences at $p < 0.05$.

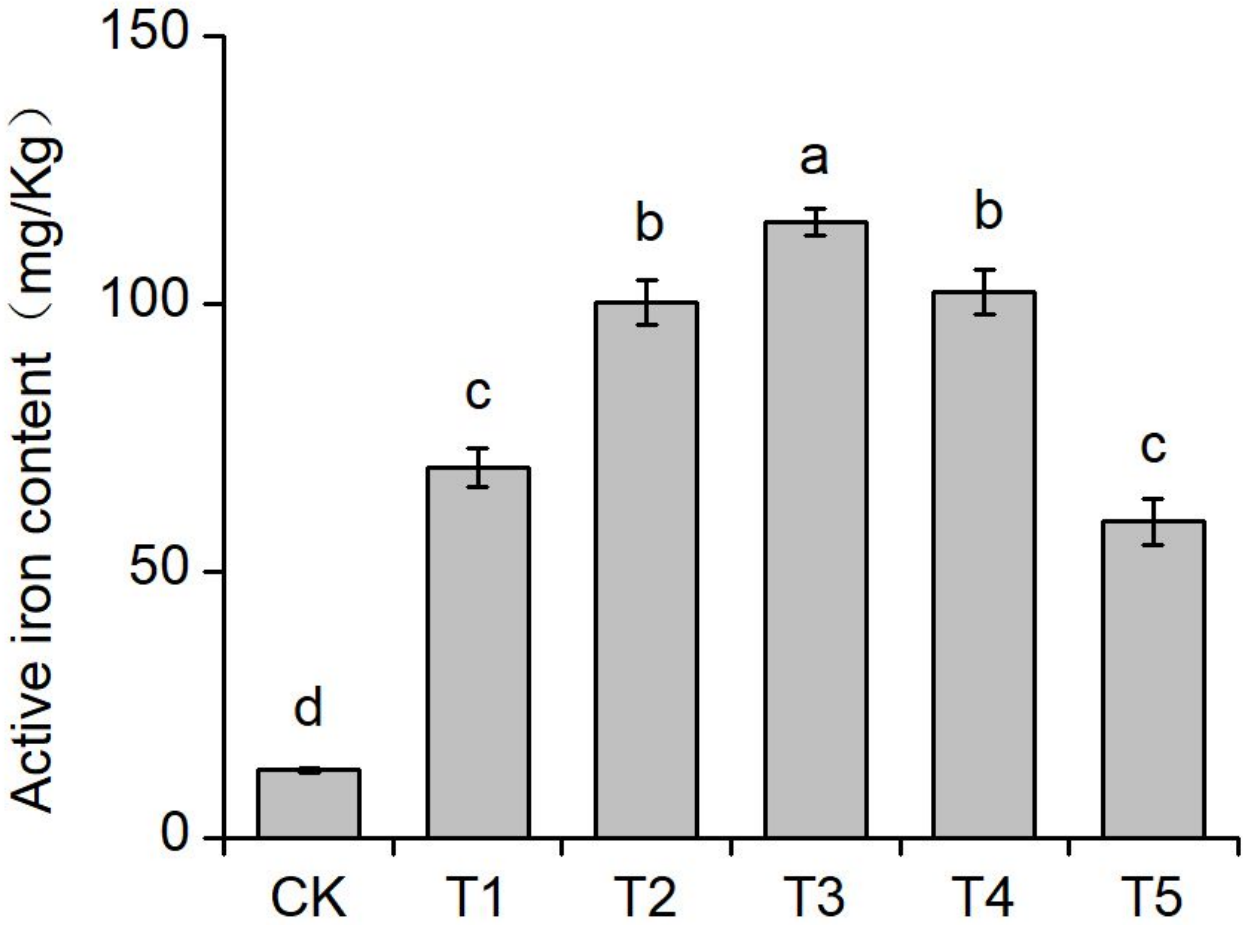

Figure 6

Active Fe contents of leaves after 72 h of treatment. CK, DI water; T1, 2 mmol/L FeSO4; NCFe (T2-T4) were prepared based on the charge ratio of NCs to Fe; T2, 1:300; T3, 1:3000; T4, 1:30000; T5, 2 mmol/L Fe-EDTA. Means with different letters represent significant differences at $p < 0.05$.

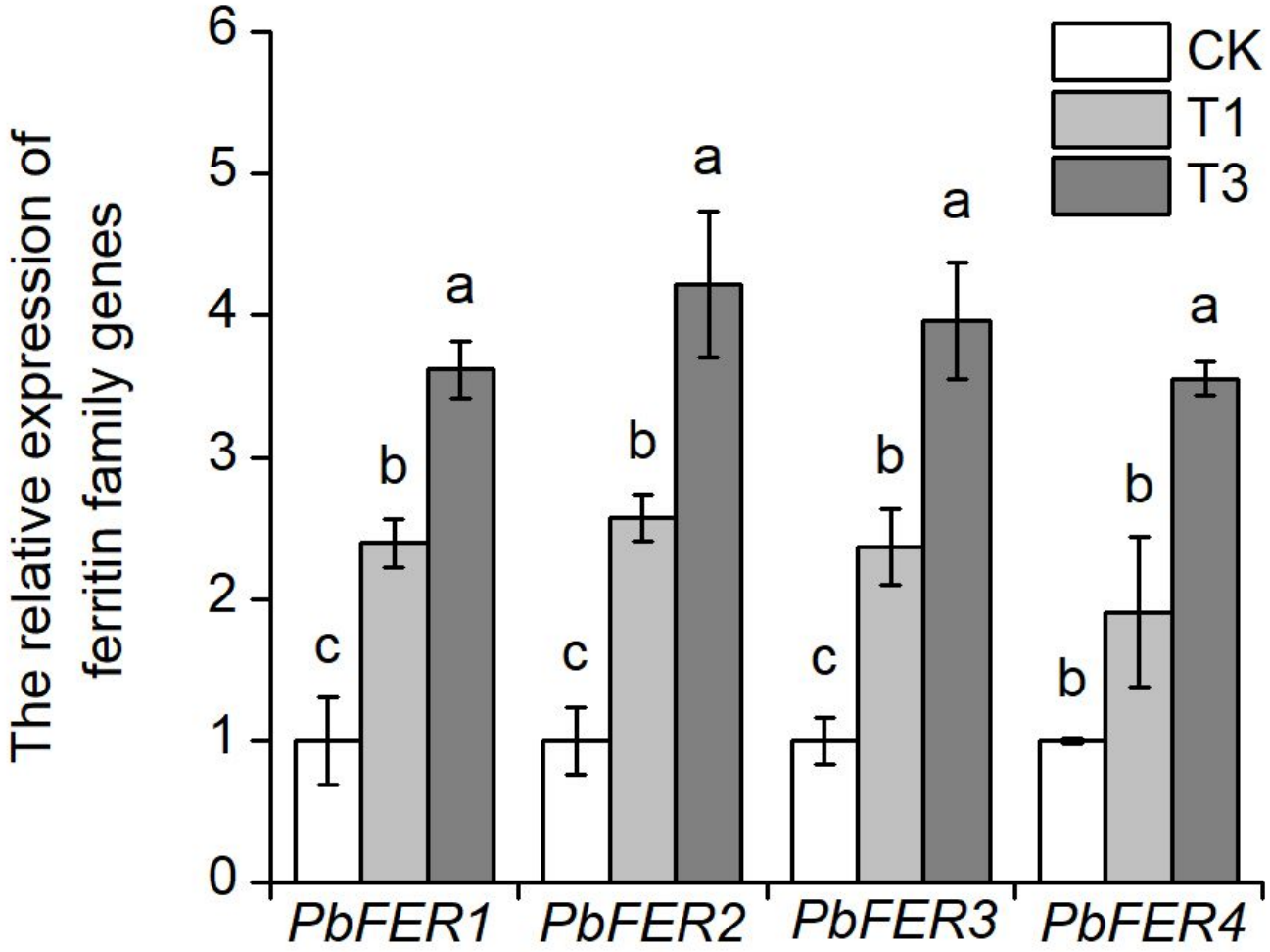

Figure 7

Relative expression levels of ferritin family genes in leaves after 72 h of treatment. CK, DI water; T1, 2 mmol/L FeSO4; T2: chelate prepared at a NC-to-Fe charge ratio of 1:3000. All suspensions were diluted with DI water. Means followed by different letters present significant differences at $p < 0.05$.

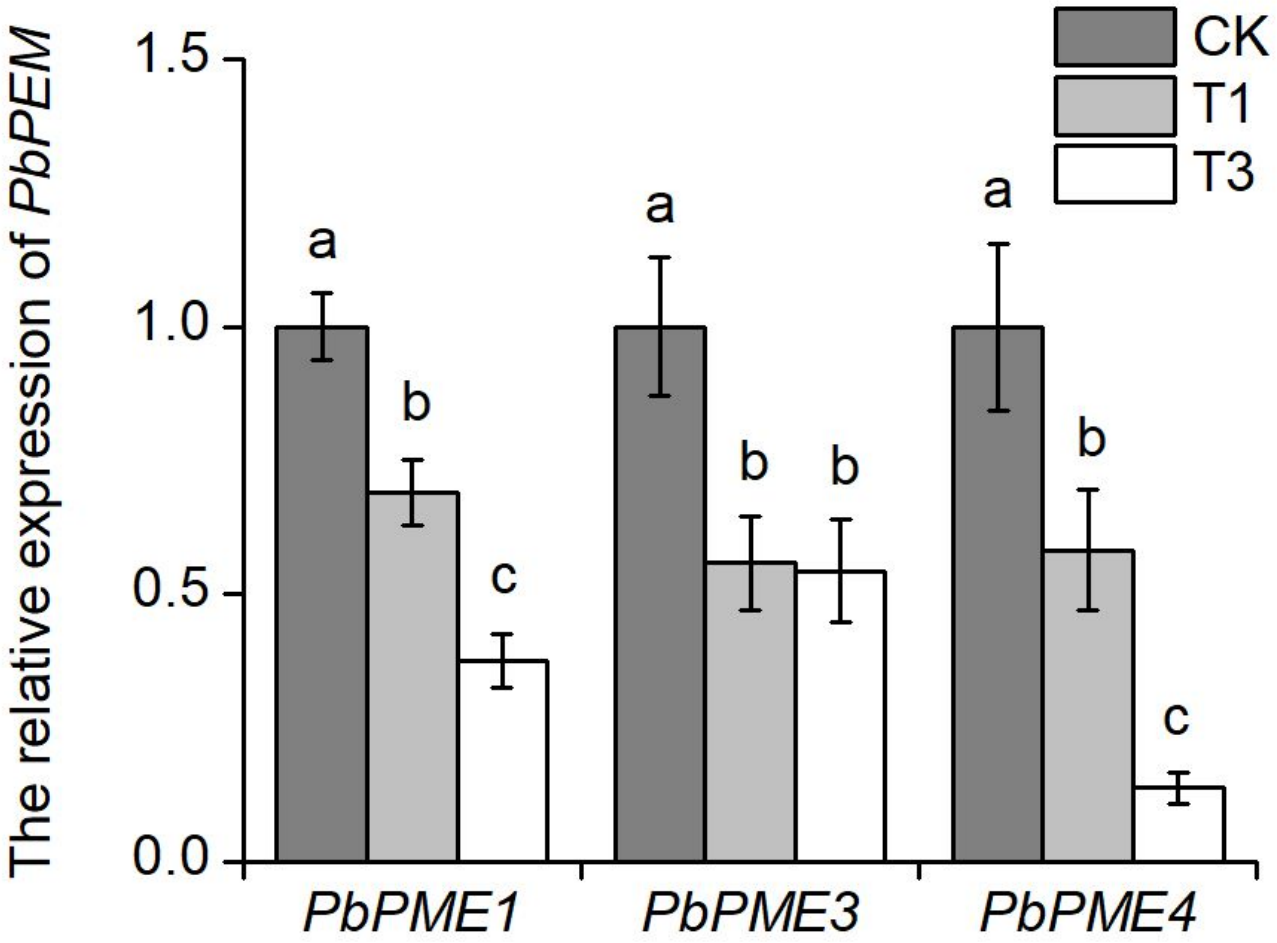

Figure 8

Relative expression of the pectin methylesterase gene in leaves after 72 h of treatment. CK, DI water; T1, 2 mmol/L FeSO4; T2: chelate prepared with a NC-to-Fe charge ratio of 1:3000. All suspensions were diluted with DI water. Means followed by different letters present significant differences at $p < 0.05$.

Supplementary Files

This is a list of supplementary files associated with this preprint. Click to download.

- EffectsofNCFeonFluorescentparameters.docx